# Correcting 19th and 20th century sea surface temperatures improves simulations of Atlantic hurricane activity

Duo Chan[1*], Gabriel A. Vecchi[2], Wenchang Yang[2], and Peter Huybers[1]

duochan@g.harvard.edu

[1]*Department of Earth and Planetary Sciences, Harvard University USA*

[2]*Department of Geosciences, Princeton University USA*

**Changes in the statistics of North Atlantic hurricanes are known to depend upon the pattern of tropical sea surface temperatures (SSTs). Dynamical and statistical models are key tools to predict future hurricane activity, with our confidence in this application rooted in the models' ability to skillfully reproduce hurricane variations over the past 30-40 years, when satellite data allows accurate reconstruction of observed ocean temperature variations. Extending the evaluation of simulations forced with historical SSTs against hurricane activity to century scales provides a more complete assessment of predictive skill, but which is limited in part by uncertainty in historical SST estimates. Here we show that recent corrections for systematic offsets in bucket SST measurements improve model skill in recovering North Atlantic hurricane counts and lead to consistent reproducibility since the late 19th century. Changes in hurricane frequency introduced by revising historical SST data are of similar magnitude to projected changes for 2081-2100 in response to increasing greenhouse gases, highlighting the importance of accurately assessing SST patterns for purposes of both historical and future predictions.**

Changes in Atlantic hurricane activity in response to climate variations remain uncertain[1,2] but have major societal implications[3,4]. Available historical records show substantial multidecadal variations in Atlantic hurricane activity[5] that covary with SST differences between the Atlantic main development region and the remainder of the Tropics[6,7]. Both statistical[5,6,14] and dynamical models[7] are skillful in reproducing variations in observational estimates of hurricane frequency over recent decades. Such covariation supports an interpretation that SST variations are a proxy for variations in hurricane available potential energy associated with the temperature difference between the surface and Tropical tropopause[5,8,9]. When extended to cover the late 19th and the full 20th century with commonly-used reconstructions of SSTs, however, models fail to capture the amplitude of multi-decadal variations in reconstructed hurricane counts. For example, statistical models based on tropical SST differences predict hurricane activities that are weaker than observed during the late 19th century and stronger in the middle of the 20th century[6,7]. Similar discrepancies arise when we simulate hurricanes using a high-resolution dynamical atmospheric model[10] and HadISST1[11] historical SST estimates (Fig. 1a).

Discrepancies in the long-term relationship between reconstructed and modeled Atlantic hurricane counts may arise for a variety of reasons. Such discrepancies could reflect errors in historical hurricane reconstructions. For example, prior to the satellite era, hurricane reconstructions must be corrected for missed events, a process that is inevitably uncertain[5,6]. Even in the satellite era, the classification of hurricanes can be uncertain on account of errors in maximum wind speed estimates[12]. A framework of reproducing hurricane activity solely on the basis of historical SST variations is also suspect. For example, upper-level atmospheric conditions have the potential to evolve independently of SSTs[13,14]. Recent simulations also indicate that hurricane frequency decreases with increasing $CO_2$ independent of an SST influence[15]. An additional possibility, which is the focus here, is that errors in SST estimates corrupt past simulation skill.

All widely-used estimates of historical SST variability depend upon in situ observations compiled in the International Comprehensive Ocean-Atmosphere Data Set[16,17] (ICOADS, Fig. 2a). This data requires corrections to account for temporal and spatial inhomogeneity in measurement strategies[18–20]. Prior to the 1980s, data comes largely from measurements made using buckets, comprising 40% of observations between 1942-1981 and 95% of observations prior to 1942[21]. Bucket temperatures are estimated to be, on average, biased 0.5°C toward cooler temperatures over the early 20th century[22] foremost because of cooling from wind-induced evaporation[20]. Other biases are also present, however, such as heating of a bucket by the sun[22,23], and the degree to which cooling and heating influences temperature observations depends upon the design of a bucket and measurement protocols.

Lack of metadata by which to make specific corrections has necessitated simplifying assumptions regarding the spatial and temporal structure of bucket biases. HadISST1, for example, uses globally uniform and linear weights to represent a transition from wooden buckets to less-insulated canvas buckets[11]. Since hurricanes and other climate phenomena are sensitive to patterns of tropical SST changes[5,24,25], however, correctly diagnosing the spatio-temporal evolution of these biases could be important. A recently developed method allows for intercomparison of nearby SST measurements to identify systematic offsets among various groups of ships[26] and for correction of regional SST biases in accord with the uneven spatial and temporal sampling of individual ship groups. These biases range between $\pm 0.5°C$ and their correction gives a more globally homogeneous pattern of warming over the early 20th century that is in better agreement with near-shore measurements of surface atmospheric temperature[27].

More specifically, groupwise SST corrections lead to a warming of the Tropical Atlantic, and a general cooling elsewhere in the Tropics in the late 19th century (Fig. 2c). A hurricane-permitting atmospheric model that skillfully recovers many aspects of hurricane climatology[10] (Fig. 2b) indicates that these late-19th century SST corrections substantially impact hurricane simulations across the globe (Fig. 2d).

Groupwise SST corrections also lead to revisions in multidecadal variations of SST differences between the Atlantic main development region and the tropical average across the 19th and 20th century (Fig. 3, see ”relative SST index” in methods). Correction of SST data coming from Germany, Netherlands, and a group of data whose nationality is unknown and is referred to as deck number 156 makes the main development region warmer between 1880-1930. Between 1930 and 1960 British and Germany SST corrections result in colder SSTs in the main development region, whereas Japanese and Netherlands SST corrections give warmer SSTs over Tropical oceans and, therefore, a decrease in the relative SST difference. To quantitatively explore implications of groupwise corrections to SSTs for hurricane simulations, we correct HadISST1 for groupwise bucket offsets, referred to as HadISST1b, and perform a paired suite of hurricane permitting model simulations spanning 1871-2019 using this revised SST dataset. Our reference experiment set is, on the other hand, forced with HadISST1.

Changes in hurricane counts between the atmospheric model experiment forced with HadISST1 and with HadISST1b (Fig. 1c) are consistent with corrections in the relative SST index (Fig. 3). The HadISST1b-forced simulations yield increased Atlantic hurricane activity in the late 19th century (Fig. 1d, Fig. 2d) and decreased activity in the middle 20th century (Fig. 1c) and reproduce multi-decadal variations in better accord with the historical reconstruction (Fig. 1b). The explained variance (square of Pearson's correlation, $r^2$) for 15-year running averaged counts increases significantly ($P$ <0.05) from 0.21 between observations and HadISST1-based simulations to 0.44 between observations and HadISST1b-based simulations (Extended Data Fig. 1). A complimentary statistic, the root-mean-square error (RMSE), decreases significantly (P ¡0.05) from 1.06 hurricanes per year between observations and simulations with HadISST1 to 0.83 between observations and simulations with HadISST1b ($P$ <0.05) throughout 1885-2011. Whereas the RMSE of 1.06 with HadISST1 is exceptionally unlikely ($P$ <0.01) to arise solely from atmospheric internal variability, errors in hurricane adjustments and previously reported SST uncertainties, the RMSE of 0.83 with HadISST1b ($P$ =0.1, Extended Data Fig. 2) is less obviously inconsistent with known errors. Improvements in model's reproduction skill are robust to how we calibrate the model or smooth time series (Table 1).

Hurricane simulations using HadISST1b also give greater consistency between the number of observed and simulated hurricane counts in individual active and inactive periods, especially prior to the satellite era (Fig. 1d). For the active period spanning 1885-1899, simulations using

HadISST1 yield, on average, 6.8±0.5 (2 s.d. error) hurricanes per year, an activity that is significantly less ($P$ <0.05) than the value of 8.4±1.3 from observational estimates. Predictions using HadISST1b, however, are consistent with observations at 8.0±0.8 hurricanes per year. During the next active period, between 1930-1959, simulations using HadISST1 yield 8.3±0.3 hurricanes per year, a value that is significantly higher ($P$ <0.05) than the observed value of 6.9±0.9 hurricanes per year, whereas simulations using HadISST1b yield a more observationally consistent 7.6±0.4 hurricanes per year.

Further quantification of agreement between simulated and observed hurricanes comes from a 40-year running York regression of simulated to observed hurricane counts, $N_s = \alpha N_o + \beta$. $N_s$ and $N_o$ are, respectively, unsmoothed simulated and observed Atlantic hurricane counts. If model simulations perfectly follow observational estimates, $\alpha$ equals one. On average, $\alpha$ is 1.18 over the 20th century with HadISST1 but decreases to 0.91 with HadISST1b (Fig. 4a), indicating more consistent model simulations and observed hurricane counts after accounting for groupwise SST offsets. Moreover, $\alpha$ is more stable using HadISST1b. Quantitatively, the variation of $\alpha$ across years is 0.33 (1 s.d.) with HadISST1 and decreases to 0.16 with HadISST1b. Specifically, simulations with HadISST1b not exhibiting a peak of 1.85 in the 1920s that appears when using HadISST1 (Fig. 4a-b). The peak comes from a rapid increase in simulated hurricane counts between 1920 to 1940 (Fig. 1a) that is moderated when forcing the model with HadISST1b (Fig. 1b). The rapid increase in HadISST1-based simulations involves biases in Deutsche Seewarte Marine data over the Atlantic main development region and the Japanese Kobe Collection over the Pacific (Fig. 3). Whereas German temperatures have an offset becoming 0.33°C warmer from 1920 to 1941, the Japanese temperatures involve a 0.35°C drop in the 1930s because of a truncation error[26]. As a result, the relative SST index experiences an artificial increase from 1920-1940 in ICOADS that underlies all major historical SST estimates, including HadISST1. Correcting for the national offsets decreases $\alpha$ to 0.82 with HadISST1b (Fig. 4c).

Groupwise bucket SST corrections significantly improve simulated decadal variability of North Atlantic hurricane counts. There still appears scope for further reducing discrepancies between observed and model-reproduced hurricane counts, including those spanning the transition to the satellite era in the early 1980s, through further improving the accuracy of historical SST data in two respects. First, engine-room-intake measurements of SST, which are more prevalent in the second half of the 20th century, are potentially subject to systematic biases associated with changes in depth of sampling, engine room design, and conversion to hull-mounted sensors[18]. Groupwise offsets have, however, not yet been developed for engine-room-intake measurements. Second, SST biases associated with individual ships may also contribute substantial uncertainty to regional SST patterns[28,29]. That is, offsets in ICOADSb are estimated and corrected after averaging ships coming from the same nation and data-collecting groups[27], but ships within the same group may have distinct SST biases that depend on sampling characteristics or ship design.

Further reduction in discrepancies could also come from improving historical hurricane reconstructions or climate models. For example, reconstructions of historical hurricane counts could be further improved as more historical ship logs are rescued[5,17]. It would also be useful to estimate uncertainties in the HURDAT2 dataset associated, for example, with classification errors arising from uncertainties in wind speed estimates[12]. Climate models could be further improved through better resolving the structure of hurricanes and large-scale climate processes that influence hurricane activity and more fully incorporating relevant physical processes and environmental factors[15].

Our major finding is that biases in historical SST patterns are a dominant limiting factor in the ability of models to recover historical Atlantic hurricane counts at decadal timescales. The more stable relationship between observed and simulated hurricane activity found using HadISST1b supports the feasibility of accurate predictions of future hurricane activity based upon evolving SST patterns[30–33]. More importantly, revisions to historical bucket SSTs lead to an 18% increase in hurricane activity between 1885-1920 in the North Atlantic (Fig. 2d). This change is larger in magnitude than the multi-model expected decrease in hurricane frequency of 3% in the North Atlantic simulated in response to projected 21st century warming in the RCP4.5 scenario[34] (Extended Data Fig. 3) and of comparable magnitude to the simulated 24% reduction in the Northwest Pacific, the region having the largest predicted changes. Such a strong historical sensitivity of hurricane statistics to regional SSTs also highlights the importance of accurately predicting patterns of future SST change for purposes of accurate hurricane projections[35].

1. Knutson, T. *et al.* Tropical cyclones and climate change assessment: Part II. projected response to anthropogenic warming. *Bulletin of the American Meteorological Society* (2019).

2. Cha, E. J., Knutson, T. R., Lee, T.-C., Ying, M. & Nakaegawa, T. Third assessment on impacts of climate change on tropical cyclones in the typhoon committee region—Part II:

Future projections. *Tropical Cyclone Research and Review* (2020).

3. Pielke Jr, R. A. *et al.* Normalized hurricane damage in the united states: 1900–2005. *Natural Hazards Review* **9**, 29–42 (2008).

4. Emanuel, K. Global warming effects on us hurricane damage. *Weather, Climate, and Society* **3**, 261–268 (2011).

5. Vecchi, G. A. & Knutson, T. R. On estimates of historical North Atlantic tropical cyclone activity. *Journal of Climate* **21**, 3580–3600 (2008).

6. Vecchi, G. A. & Knutson, T. R. Estimating annual numbers of Atlantic hurricanes missing from the HURDAT database (1878–1965) using ship track density. *Journal of Climate* **24**, 1736–1746 (2011).

7. Caron, L.-P. *et al.* How skillful are the multiannual forecasts of Atlantic hurricane activity? *Bulletin of the American Meteorological Society* **99**, 403–413 (2018).

8. Emanuel, K. A. The maximum intensity of hurricanes. *Journal of the Atmospheric Sciences* **45**, 1143–1155 (1988).

9. Sobel, A. H., Nilsson, J. & Polvani, L. M. The weak temperature gradient approximation and balanced tropical moisture waves. *Journal of the Atmospheric Sciences* **58**, 3650–3665 (2001).

10. Zhao, M., Held, I. M., Lin, S.-J. & Vecchi, G. A. Simulations of global hurricane climatology, interannual variability, and response to global warming using a 50-km resolution GCM. *Journal of Climate* **22**, 6653–6678 (2009).

11. Rayner, N. *et al.* Global analyses of sea surface temperature, sea ice, and night marine air temperature since the late nineteenth century. *Journal of Geophysical Research: Atmospheres* **108** (2003).

12. Landsea, C. W. *et al.* A reanalysis of the 1921–30 Atlantic hurricane database. *Journal of Climate* **25**, 865–885 (2012).

13. Emanuel, K., Solomon, S., Folini, D., Davis, S. & Cagnazzo, C. Influence of tropical tropopause layer cooling on Atlantic hurricane activity. *Journal of Climate* **26**, 2288–2301 (2013).

14. Vecchi, G. A. *et al.* Multiyear predictions of North Atlantic hurricane frequency: Promise and limitations. *Journal of Climate* **26**, 5337–5357 (2013).

15. Vecchi, G. A. *et al.* Tropical cyclone sensitivities to CO2 doubling: roles of atmospheric resolution, synoptic variability and background climate changes. *Climate Dynamics* **53**, 5999–6033 (2019).

16. Woodruff, S., Diaz, H., Elms, J. & Worley, S. COADS release 2 data and metadata enhancements for improvements of marine surface flux fields. *Physics and Chemistry of the Earth* **23**, 517–526 (1998).

17. Freeman, E. *et al.* ICOADS Release 3.0: a major update to the historical marine climate record. *International Journal of Climatology* **37**, 2211–2232 (2017).

18. Kent, E. C. *et al.* A call for new approaches to quantifying biases in observations of sea surface temperature. *Bulletin of the American Meteorological Society* **98**, 1601–1616 (2017).

19. Kent, E. C. *et al.* Observing requirements for long-term climate records at the ocean surface. *Frontiers in Marine Science* **6**, 441 (2019).

20. Folland, C. & Parker, D. Correction of instrumental biases in historical sea surface temperature data. *Quarterly Journal of the Royal Meteorological Society* **121**, 319–367 (1995).

21. Kennedy, J., Rayner, N., Smith, R., Parker, D. & Saunby, M. Reassessing biases and other uncertainties in sea surface temperature observations measured in situ since 1850: 2. biases and homogenization. *Journal of Geophysical Research: Atmospheres* **116** (2011).

22. Kennedy, J., Rayner, N., Atkinson, C. & Killick, R. An ensemble data set of sea surface temperature change from 1850: The Met Office Hadley Centre HadSST. 4.0.0.0 data set. *Journal of Geophysical Research: Atmospheres* **124**, 7719–7763 (2019).

23. Carella, G. *et al.* Estimating sea surface temperature measurement methods using characteristic differences in the diurnal cycle. *Geophysical Research Letters* **45**, 363–371 (2018).

24. Vecchi, G. A. *et al.* Statistical–dynamical predictions of seasonal north atlantic hurricane activity. *Monthly Weather Review* **139**, 1070–1082 (2011).

25. Xie, S.-P. *et al.* Global warming pattern formation: Sea surface temperature and rainfall. *Journal of Climate* **23**, 966–986 (2010).

26. Chan, D. & Huybers, P. Systematic differences in bucket sea surface temperature measurements amongst nations identified using a linear-mixed-effect method. *Journal of Climate* (2019).

27. Chan, D., Kent, E. C., Berry, D. I. & Huybers, P. Correcting datasets leads to more homogeneous early-twentieth-century sea surface warming. *Nature* **571**, 393 (2019).

28. Kent, E. & Berry, D. Assessment of the marine observing system (ASMOS): final report (2008).

29. Kennedy, J., Smith, R. & Rayner, N. Using AATSR data to assess the quality of in situ sea-surface temperature observations for climate studies. *Remote Sensing of Environment* **116**, 79–92 (2012).

30. Emanuel, K., Sundararajan, R. & Williams, J. Hurricanes and global warming: Results from downscaling IPCC AR4 simulations. *Bulletin of the American Meteorological Society* **89**, 347–368 (2008).

31. Mendelsohn, R., Emanuel, K., Chonabayashi, S. & Bakkensen, L. The impact of climate change on global tropical cyclone damage. *Nature Climate Change* **2**, 205–209 (2012).

32. Emanuel, K. A. Downscaling CMIP5 climate models shows increased tropical cyclone activity over the 21st century. *Proceedings of the National Academy of Sciences* **110**, 12219–12224 (2013).

33. Sobel, A. H. *et al.* Tropical cyclone hazard to Mumbai in the recent historical climate. *Monthly Weather Review* **147**, 2355–2366 (2019).

34. Bhatia, K., Vecchi, G., Murakami, H., Underwood, S. & Kossin, J. Projected response of tropical cyclone intensity and intensification in a global climate model. *Journal of Climate* **31**, 8281–8303 (2018).

35. Christensen, J. H. *et al.* Climate phenomena and their relevance for future regional climate change. In *Climate Change 2013 the Physical Science Basis: Working Group I Contribution to the Fifth Assessment Report of the Intergovernmental Panel on Climate Change*, 1217–1308 (Cambridge University Press, 2013).

36. York, D., Evensen, N. M., Martınez, M. L. & De Basabe Delgado, J. Unified equations for the slope, intercept, and standard errors of the best straight line. *American Journal of Physics* **72**, 367–375 (2004).

**Acknowledgements** D.C. and P.H. are funded by a grant from the Harvard Global Institute. G.A.B. and W.Y. are funded by NOAA grant NA180AR4320123 and the Carbon Mitigation Initiative at Princeton University. The simulations presented in this article were performed on computational resources managed and supported by Princeton Research Computing, a consortium of groups including the Princeton Institute for Computational Science and Engineering (PICSciE) and the Office of Information Technology's High Performance Computing Center and Visualization Laboratory at Princeton University. The model used in this study (HiRAM) was developed at NOAA/GFDL, and is made freely available at https://www.gfdl.noaa.gov/hiram-quickstart/.

**Author contributions** D.C., G.A.V., and P.H. conceived and designed the study. D.C. developed HadISST1b and G.A.V. and W.Y. performed HiRAM simulations. D.C. led the analysis and writing. All authors contributed to interpreting results and discussed the manuscript.

**Competing interests** The authors declare that they have no competing financial interests.

**Correspondence and requests for materials** should be addressed to D.C.

**Table 1.** Model skill in reproducing historical North Atlantic hurricane counts.

| Length of smoothing window | Calibration method | $r^2$ HadISST1 | $r^2$ HadISST1b | RMSE HadISST1 | RMSE HadISST1b |
|---|---|---|---|---|---|
| 15 | add 1.1 | 0.21 | $0.44^{*}$ | 1.06 | $0.83^{*}$ |
| 15 | scale by 1.2 | 0.21 | $0.44^{*}$ | 1.19 | $0.90^{*}$ |
| 15 | add 1.1; splice | 0.21 | $0.45^{*}$ | 1.06 | $0.81^{*}$ |
| 25 | add 1.1 | 0.21 | $0.38^{**}$ | 0.90 | $0.74^{**}$ |

Shown statistics are squared Pearson's correlation coefficient, $r^2$, and root-mean-square-error, RMSE, between observational and ensemble-mean of simulated hurricane counts using hadISST1 and HadISST1b. We explore the sensitivity of results by performing different smoothing (15-year or 25-year), different model calibrations (add model results with 1.1 or scale model results by 1.2), and turning off SST corrections in the satellite era (splice, see methods). Results are for 1878-2018 but where an interval equal to half that of the smoothing window is omitted from the beginning and end. Significant increases in $r^2$ or decreases in RMSE relative to the HadISST1 case are indicated using a "*"($P$ <0.05) or "**" ($P$ <0.1). Significance is evaluated using a Monte Carlo technique (see methods).

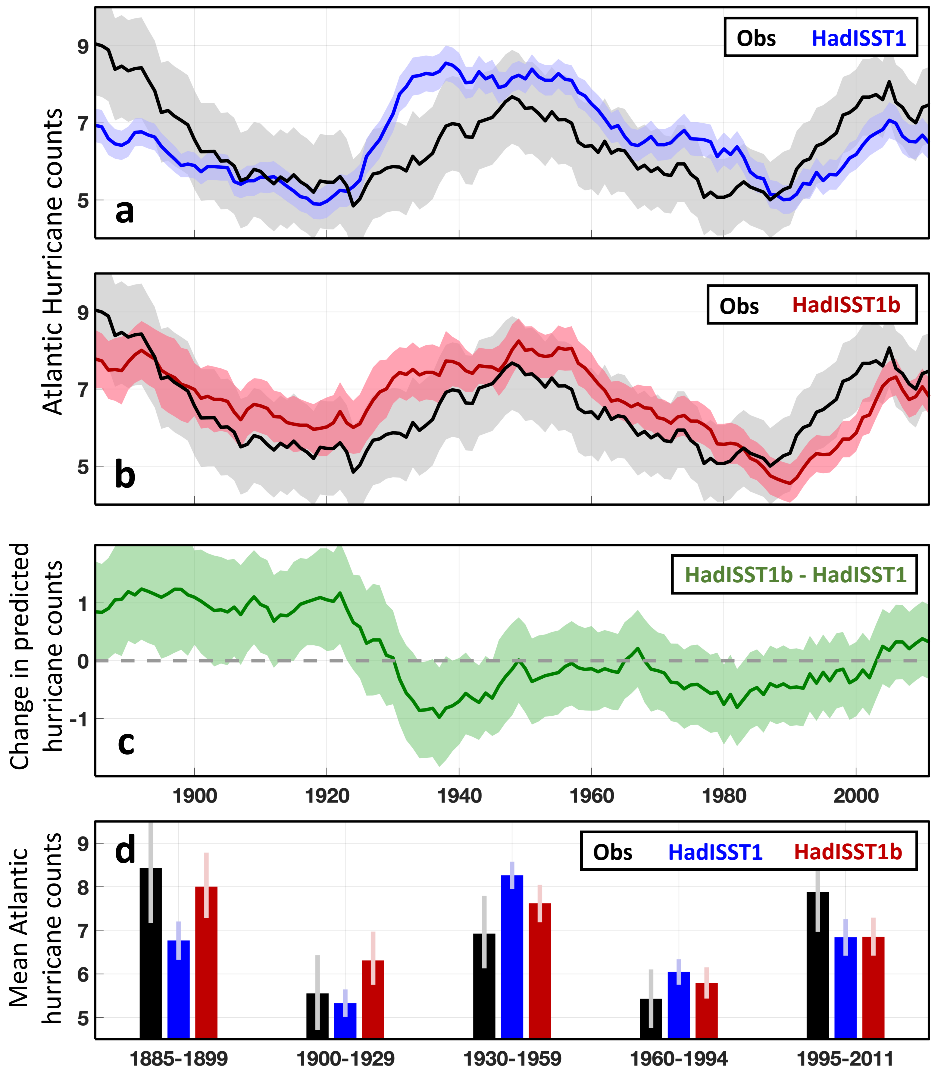


**Fig. 1. Observed and simulated Atlantic hurricane counts. a**. Simulations using HadISST1 give significantly lower hurricane counts in the late 19th century than observational estimates ($P$ <0.05), and higher counts in the middle 20th century ($P$ <0.05). **b**. Simulated and observed hurricane counts become consistent using HadISST1b, which includes corrections for groupwise SST offsets. **c**. Difference in predicted hurricane counts between simulations using HadISST1 and HadISST1b. Uncertainties are shown atmospheric for internal variability and uncertainties in hurricane adjustments added in quadrature (gray shading in panels a-b, 95%

C.I.), atmospheric internal variability (blue shading in panel a, 95% C.I.), and atmospheric internal variability and uncertainties arising from uncertain SST corrections added in quadrature (red shading, 95% C.I.). Curves in a-c are 15-year running averages with the initial (1878-1884) and final (2012-2018) 7 years truncated. **b**. Average hurricane counts over active and inactive periods where uncertainties (vertical bars, 95% C.I.) correspond to those in **a** and **b**.

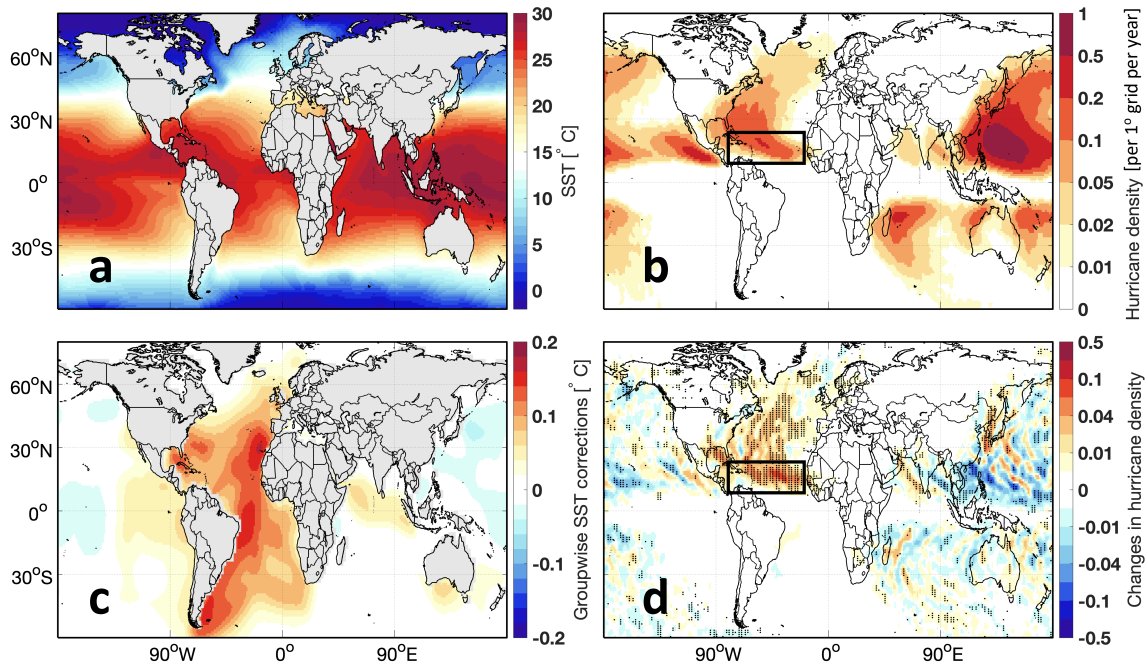


**Fig. 2. Sea surface temperature and simulated hurricane counts. a**. Climatological SST over 1885-1920 in HadISST1. **b**. The ensemble-mean hurricane track density averaged over 1885-1920 in simulations with HadISST1. The Atlantic main development region is highlighted (black box). **c**. Groupwise SST corrections averaged over 1885-1920 as incorporated in HadISST1b, and **d**. associated ensemble-mean changes in hurricane density. Accounting for groupwise SST offsets significantly increases hurricane density in the North Atlantic (dots, $P$ <0.05, two-sample t-testn, N = 36). For visualization purpose, hurricane track density on $1^{\circ}$ gridding is smoothed using a nine-grid 2D convolutional smoother.

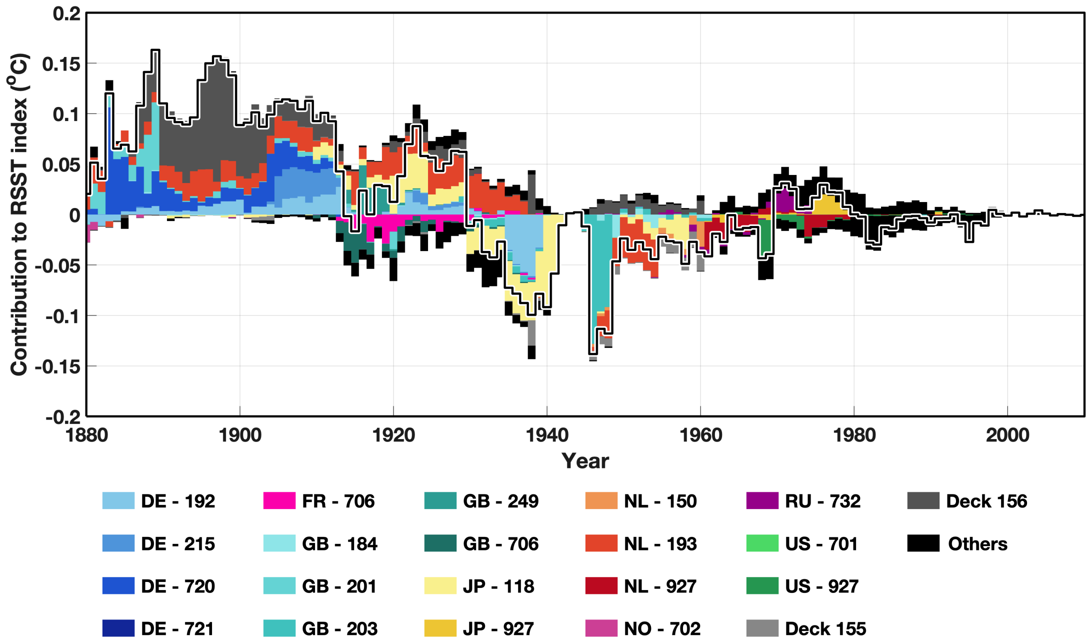


**Fig. 3. Groupwise decomposition of SST corrections in HadISST1b.** Contributions from individual groups to corrections in the relative SST index (black line). Relative SST index is a weighted difference between SST anomalies in the main development region and the entire Tropics[14] (also see methods). Groups are designated according to nation (two letter acronyms) and deck number, where deck is an indicator of marine data collectors in ICOADS[17]. Nation abbreviations are for Germany (DE), Great Britain (GB), Japan (JP), the Netherlands (NL), Russia (RU), and the United States (US). Note that the magnitude of corrections incorporated in HadISST1b trends toward lower magnitudes with time because, whereas ICOADSb is a bucket-only SST product, HadISST1b corrections are scaled by the fraction of bucket versus other measurements in individual grid boxes over time.

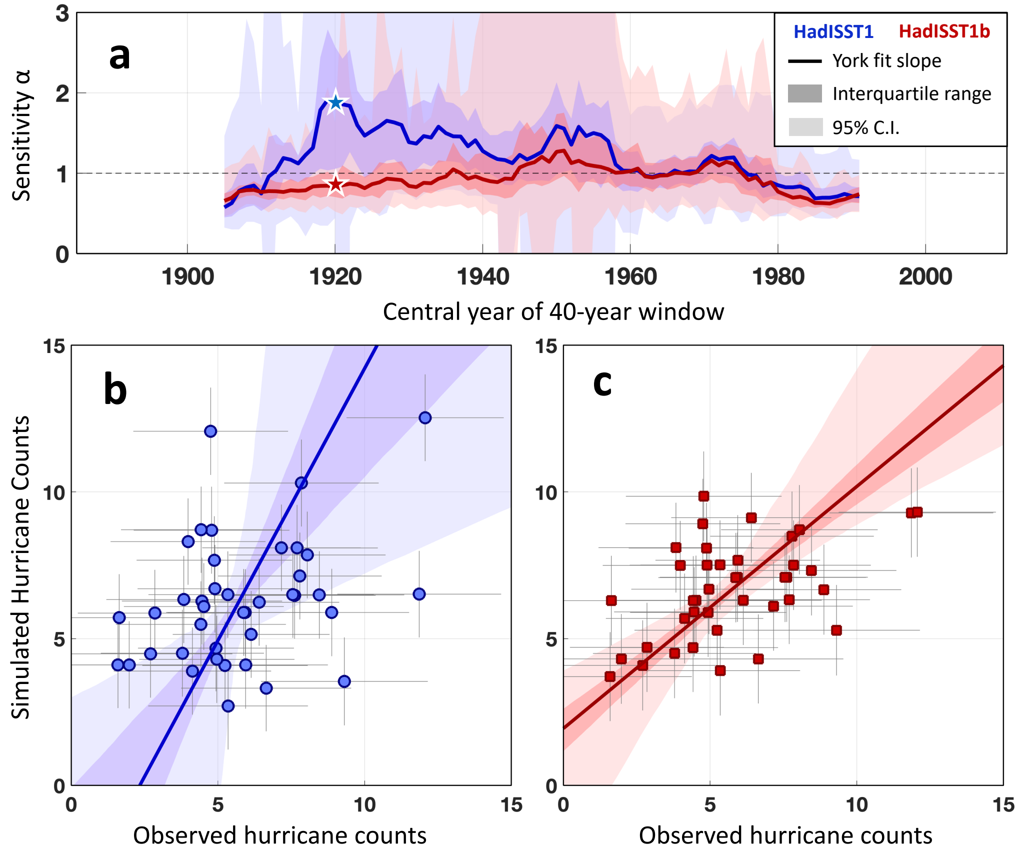


**Fig. 4. Regressions of simulated against observed Atlantic hurricane counts. a**. Correcting for groupwise SST offsets leads to a more stable regression slope with HadISST1b (red) than HadISST1 (blue) throughout 1885-2011. Regressions are based on unsmoothed counts using a York method[36] and are performed with a 40-year window that slides annually from 1885-1924 to 1972-2011. Regression slopes uncertainties are estimated using bootstrapping (dark shading is the interquartile range; light shading the 95% C.I., see methods). **b-c**. Details of York regressions using simulations with HadISST1 (**b**) and HadISST1b (**c**) over 1901-1940 (stars in **a**). York regressions account for uncertainties associated with interannual variability and hurricane count adjustments for observations (1 s.d., horizontal bars on individual markers) and

errors associated with interannual variability and groupwise SST corrections for simulated counts (vertical bars). Error bars are the same as in **a**.

## Methods

**Observed and simulated Atlantic hurricanes:** North Atlantic hurricane observations come from the HURDAT2 dataset[37] (1878-2018). HURDAT2 is adjusted according to an estimate of missed hurricanes before 1965 by sampling satellite observations of hurricanes using ship tracks in the ICOADS dataset[6].

We explore a series of SST-forced atmospheric model simulations using the NOAA-GFDL High Resolution Atmospheric Model (HiRAM) with the finite volume cubed-sphere dynamical core at a global 50km resolution (180x180 grid points on each of the cube faces, or C180) at 32 vertical levels[10]. This model has been shown to be skillful at simulating and predicting many aspects of TC climatology[10,38] and is widely used to understand aspects of TC climatology[39–43].

Two types of experiments are used in this study, with specified monthly-mean SST as a bottom boundary condition: 1) historical SST experiments and 2) time-slice simulations.

The time-varying SST-forced experiments are five-member initial- condition ensembles initialized in 1871 forced with either the HadISST1 or the HadISST1b monthly SST values from 1871-2019. Radiative forcing changes are prescribed from the CMIP5 historical scenario from 1871-2004 and from the CMIP5 RCP4.5 scenario from 2005-2019. Simulated hurricanes are identified using a 33 m/s windspeed threshold, under which HadISST1-based HiRAM averages 5.5 hurricanes per year in the North Atlantic. A value of 1.1 is added to simulated hurricanes to bring this simulated activity in line with observations of 6.6 hurricanes per year. An alternative approach of multiplying simulated Atlantic hurricane counts by 1.2 gives consistent results in terms of improved skill coming from correcting SSTs (Table 1).

In the "time-slice" experiments, prescribed repeating monthly SST climatology is used in order to assess the mean climatic impact of climatological SST changes; this method is regularly used to understand hurricane sensitivity[39,43]. We perform two "time-slice" experiments, each of 50-year duration, using HadISST1 SST climatology averaged over 1986-2005 and using HadISST1 SST climatology averaged over 1986-2005 plus the multi-model predicted climatological SST change following RCP4.5 averaged over 2081-2100[43] (Extended Data Fig. 3). Each experiment also includes radiative forcing relevant to each time period (fixed 1990 for the late 20th century experiment and fixed 2090 for the late 21st century experiment) following the CMIP5 historical or RCP4.5 protocol.

**Relative SST index:** We adopt a relative SST index (RSST) used elsewhere[14] to simply represent the influence of variation in June-November SST to augment the more detailed results provided by the HiRAM simulations. Specifically, $\mathrm{RSST} = 1.388\mathrm{T}'_{\mathrm{MDR}} - 1.521\mathrm{T}'_{\mathrm{Trop}}$, where $\mathrm{T}'_{\mathrm{MDR}}$ is the SST averaged over the North Atlantic main development region (20-80°W, 10-25°N, box in Fig. 2b), and $\mathrm{T}'_{\mathrm{Trop}}$ is the SST averaged over Tropical oceans in general (30°S-30°N).

**Groupwise corrections of SSTs and mapping:** Bucket SSTs are biased both by evaporative cooling and solar heating[20]. The relative contributions and magnitudes of these biases depend on bucket design and measurement protocols[18,20] that may differ among subsets of SST measurements. To account for systematic differences among groups of bucket SSTs, refs.[26,27] pair nearby measurements from distinct groups and estimate systematic offsets using a linear-mixed-effect (LME) intercomparison method. Groups are designated according to nation and deck information, where 'deck' previously denoted decks of punch cards in early digitization of marine observations but is used here as an additional indicator of marine data collectors. Although decks do not necessarily indicate distinct features of the data, highly statistically significant SST differences have been detected among distinct decks coming from the same nation such that their separation is appropriate for purposes of better correcting for offsets[26].

Groupwise offsets relative to the mean of all paired SSTs are estimated using 17.8 million differenced bucket SSTs, where pairs are identified as the closest two measurements that are within 300 km and 2 days of one another. Expected differences associated with geographical distributions, the seasonal cycle, and diurnal cycles are simultaneously estimated. Offsets are then removed from individual SST measurements according to group, location, and year, yielding a gridded bucket-only SST product called ICOADSb. More details of the LME methodology are documented in ref.[26] and of ICOADSb in ref.[27].

To merge the ICOADSb corrections with HadISST1, we follow five steps. (1) Groupwise SST corrections are averaged within $2 \times 2°$ grid boxes that contain bucket measurements and correspond to the HadISST1 grid. (2) Because HadISST1 uses SST measurements from a variety of methods, not only buckets, groupwise bucket corrections are multiplied by the ratio of bucket to all SST measurements in individual grids for each month. Thus, all corrections are multiplied by a fraction that is less than or equal to one. (3) Scaled correction fields are smoothed in space using a 2D convolutional smoother with a spatial scale of 5 grid boxes. (4) Fields are interpolated to global coverage using biharmonic spline interpolation, as encoded by Matlab's griddata function using the V4 method. Finally, (5), corrections in individual boxes are tapered to zero according to an exponential decay with a 1100 km length-scale, or 10 degrees at the Equator.

It is worth noticing that HadISST1 makes use of satellite infrared observations since 1982[11]. When calculating the ratio of bucket measurements to scale groupwise corrections, we assume that the mass of satellite observations are five times of that from simultaneous buoy and drifter measurements. To assess the influence of this assumption, we turn off groupwise bucket SST corrections after 1982 and still find robust improvements in the reproduction skill of HiRAM (Table 1 and Extended Data Fig. 4).

**Uncertainties and significance:** An error model for hurricane counts, $H$, can be written as,

$$H = \mathbf{F}(\mathrm{T}) + \epsilon_i + \frac{\mathrm{d}\mathbf{F}}{\mathrm{dT}}(b_\mathrm{T} + \epsilon_\mathrm{T}) + \epsilon_o. \tag{1}$$

$\mathbf{F}$ is a process that maps SSTs, $\mathrm{T}$, to an expected hurricane count. Both systematic SST biases, $b_\mathrm{T}$, and random SST errors, $\epsilon_\mathrm{T}$, introduce uncertainties in $H$ according to $\frac{\mathrm{d}\mathbf{F}}{\mathrm{dT}}$. Hurricane counts are also subject to atmospheric internal variability, $\epsilon_i$, and, for historical observations, reconstruction errors associated with adjustment of missed hurricanes, $\epsilon_o$. This error model makes simplifying assumptions that HiRAM captures all processes relating SSTs to Atlantic hurricane counts and neglects contributions from other processes that may influence hurricane counts, such as changes in $CO_2$ concentrations[15].

Atmospheric internal variability, $\epsilon_i$, is quantified using the spread of HiRAM members around the ensemble mean. The mean standard deviation of $\epsilon_i$ over ten HiRAM simulation members (five with HadISST1 and five with HadISST1b) is 1.97 hurricanes per year. Although hurricane counts are integers and, therefore, should follow a Poisson distribution, the component associated with internal variability appears consistent with a Gaussian distribution (Extended Data Fig. 5) and is independent across years with lag-1 Pearson's $r^2$ less than 0.01. Thus, $\epsilon_i$ for observed 15-year moving averaged counts becomes 0.51 ($\frac{1.97}{\sqrt{15}}$) hurricanes per year (light gray shadings in Fig. 1a and b). For the ensemble mean of HiRAM simulations, $\epsilon_i$ will further decrease to 0.23($\frac{0.51}{\sqrt{5}}$) hurricanes per year after accounting for averaging over five ensemble members.

Errors associated with SSTs arise both from systematic and random errors. The systematic error, $\frac{\mathrm{d}\mathbf{F}}{\mathrm{dT}} b_{\mathrm{T}}$, is approximated as equaling the groupwise corrections and are directly estimated from HiRAM simulations using the ensemble-mean difference between simulations using HadISST1 and HadISST1b (green curve in Fig. 1c). Groupwise corrections in HadISST1b decrease bias but also reveal almost an order-of-magnitude larger uncertainty in regional SST patterns than previously recognized[27]. Thus, it is important to also represent contributions from random errors in groupwise corrections, $\epsilon_{\mathrm{T}}$. Because of limitations in computing resources, we estimate the random error contributions using RSST, as opposed to HIRAM, through substituting $\frac{\mathrm{d}\mathbf{F}}{\mathrm{dR_{SST}}}\epsilon_{\mathrm{R_{SST}}}$ for $\frac{\mathrm{d}\mathbf{F}}{\mathrm{dT}}\epsilon_{\mathrm{T}}$ under the assumption that the RSST index sufficiently accounts for changes in hurricane counts.

We estimate $\frac{\mathrm{d}\mathbf{F}}{\mathrm{dR_{SST}}}$ (Extended Data Fig. 6) by regressing ensemble-average changes in hurricane counts between simulations with HadISST1b and HadISST1 (green curve in Fig. 1c) against changes in RSSTs between HadISST1b and HadISST1 (black curve in Fig. 3). Meanwhile, we estimate $\epsilon_{\mathrm{R_{SST}}}$ from a 20-member ensemble obtained by realizing errors in groupwise SST corrections in keeping with their estimated standard deviations, spatial patterns, and temporal structures[26,27]. The standard error in hurricane counts arising from uncertain SST corrections averages 0.23 hurricanes per year from 1885-2011 and decreases from 0.36 hurricanes per year in the late 19th century to less than 0.1 hurricanes per year in the satellite era. Sampling errors[44] and random errors associated with individual SST measurements[45] are omitted, but because the Atlantic main development region is well sampled since the late 19th century[44], contributions from this additional uncertainty are small.

Observational uncertainties in hurricane counts, $\epsilon_o$, come from adjusting for missed storms prior to the advent of satellite observations. Adjustments are until 1965 and involve adding a correction factor to observed hurricane counts based on sampling satellite observations using ship tracks in the ICOADS dataset[5]. Uncertainty in the correction factor takes into account year of satellite data used, size of hurricanes, and the day of year a storm was paired with observations, which yields an ensemble of 27,950 adjustment time series. Uncertainty of 15-yr smoothed hurricane counts is estimated by drawing random samples from the adjustment ensemble. Specifically, for each year, 10,000 samples are randomly drawn from 27,950 possible values without replacement and under the assumption that years are independent. After smoothing the 10,000 random realizations of possible adjustments, $\epsilon_o$ is estimated to be 0.37 hurricanes per year between 1885-1964. Because of increasing numbers of ship tracks, $\epsilon_o$ decreases with time, from 0.44 hurricanes per year in the late 19th century to 0.23 hurricanes per year in the early 1960s.

When comparing difference between observations and HiRAM simulations over active and inactive periods (Fig. 1d), individual sources of errors are summed in quadrature and significance is estimated using a standard two-sample Z-test assuming errors follow Gaussian distributions. Although hurricane counts in individual years follow a Poisson distribution, errors for the ensemble mean of 15-year smoothed hurricane counts that are also subject to additional SST uncertainties are more consistent with a Gaussian distribution.

The significance of increases in model's reproduction skill, as measured by squared-cross correlation, $r^2$, and root-mean-square-error, RMSE, is assessed using a one-sided test against a null distribution assuming that corrections have no skill. The null distribution is realized using a Monte Carlo technique whereby mean difference between HadISST1- and HadISST1b-based simulations are permuted using 10-year blocks and then smoothed to generate randomized corrections. Uncertainties associated with atmospheric internal variability and hurricane counts are accounted for by realizing annual noise time-series from normal distributions having standard deviations equal to the estimated errors reported above. The $r^2$ and RMSE obtained when introducing randomized corrections are calculated for each synthetic realization, and associated null distributions are constructed using a total of 10,000 random realizations. The expected change is negative for $r^2$ and positive for RMSE because introducing perturbations having no skill will generally increase noise in reconstructions.

To estimate slopes between observed and model simulated hurricane counts (Fig. 4), we use a York regression technique[36] to account that both estimates are uncertain. The York regression accounts for uncertainties associated with interannual variability and hurricane count adjustments for observations and errors associated with interannual variability and groupwise SST corrections for simulated counts. Uncertainty of regression slopes is estimated from a 1,000-member bootstrapping ensemble that resamples 5-year blocks with replacement.

**Data availability:** HadISST1 is freely available at https://www.metoffice.gov.uk/hadobs/hadisst/data/download.html. HadISST1b and tracked hurricanes in HiRAM simulations are available from the authors upon request and will be posted on Harvard Dataverse upon publication.

**Code availability:** Code required to reproduce key results presented in this manuscript are available from the authors upon request and will be posted on Github upon publication.

37. Landsea, C. W. & Franklin, J. L. Atlantic hurricane database uncertainty and presentation of a new database format. *Monthly Weather Review* **141**, 3576–3592 (2013).

38. Zhao, M., Held, I. M. & Vecchi, G. A. Retrospective forecasts of the hurricane season using a global atmospheric model assuming persistence of SST anomalies. *Monthly Weather Review* **138**, 3858–3868 (2010).

39. Held, I. M. & Zhao, M. The response of tropical cyclone statistics to an increase in CO2 with fixed sea surface temperatures. *Journal of Climate* **24**, 5353–5364 (2011).

40. Zhao, M., Held, I. M. & Lin, S.-J. Some counterintuitive dependencies of tropical cyclone frequency on parameters in a GCM. *Journal of the Atmospheric Sciences* **69**, 2272–2283 (2012).

41. Merlis, T. M., Zhao, M. & Held, I. M. The sensitivity of hurricane frequency to ITCZ changes and radiatively forced warming in aquaplanet simulations. *Geophysical Research Letters* **40**, 4109–4114 (2013).

42. Vecchi, G. A., Fueglistaler, S., Held, I. M., Knutson, T. R. & Zhao, M. Impacts of atmospheric temperature trends on tropical cyclone activity. *Journal of Climate* **26**, 3877–3891 (2013).

43. Knutson, T. R. *et al.* Global projections of intense tropical cyclone activity for the late twenty-first century from dynamical downscaling of CMIP5/RCP4. 5 scenarios. *Journal of Climate* **28**, 7203–7224 (2015).

44. Kennedy, J., Rayner, N., Smith, R., Parker, D. & Saunby, M. Reassessing biases and other uncertainties in sea surface temperature observations measured in situ since 1850: 1. mea-

surement and sampling uncertainties. *Journal of Geophysical Research: Atmospheres* **116** (2011).

45. Kent, E. C. & Challenor, P. G. Toward estimating climatic trends in SST. Part II: Random errors. *Journal of Atmospheric and Oceanic Technology* **23**, 476–486 (2006).

46. Van Vuuren, D. P. *et al.* The representative concentration pathways: an overview. *Climatic Change* **109**, 5 (2011).

496 **Extended Data Figures**

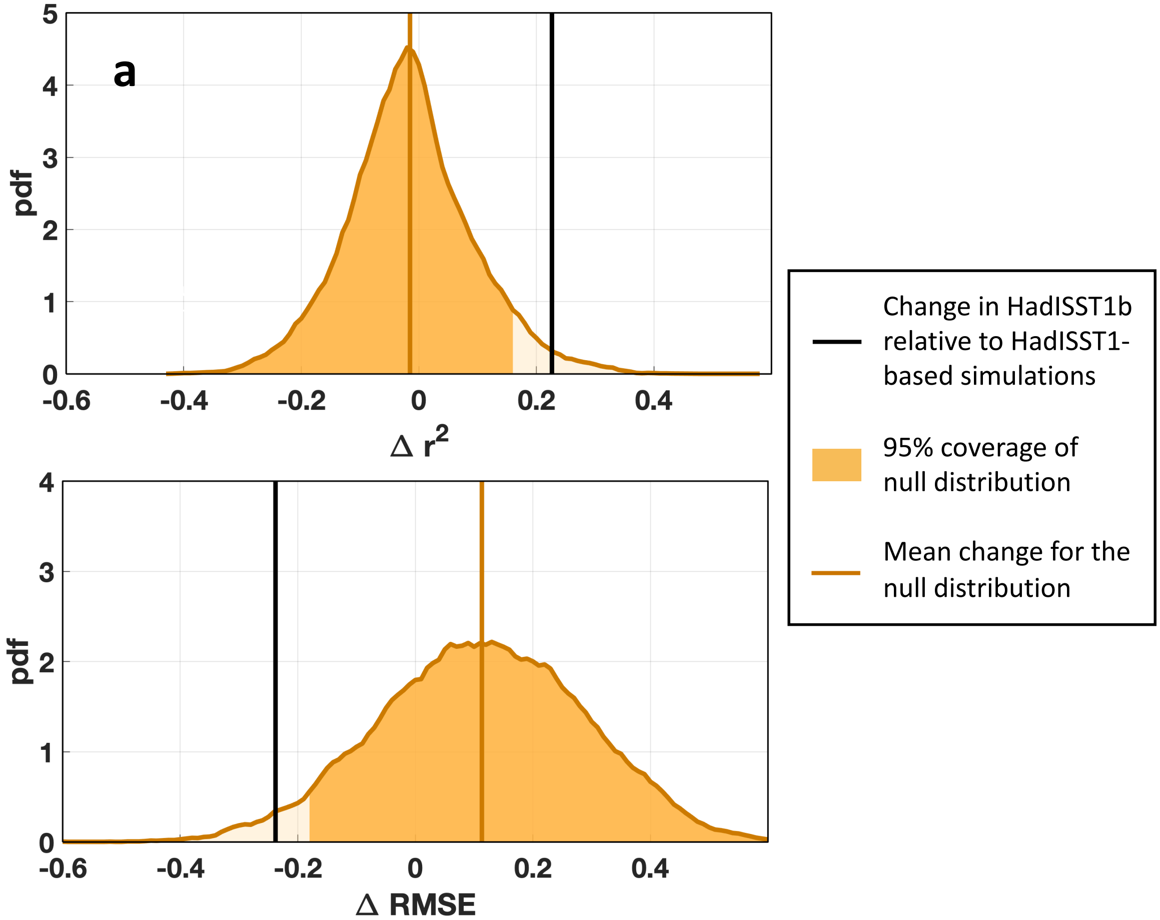


497

498 **Extended Data Fig. 1. Significant improvements in model's reproduction skills.** Compared
499 with HadISST1-based simulations, accounting for groupwise corrections significantly ($P<0.05$)
500 increases correlation ($r^2$) and decreases RMSE with observed hurricane counts. Reproduction skills
501 are evaluated using 15-year running averaged counts from 1885 to 2011. The null distribution of
502 no improvement in reproduction skills (golden) is constructed using a Monte Carlo method that
503 makes random corrections to HadISST1-based simulations (see methods).

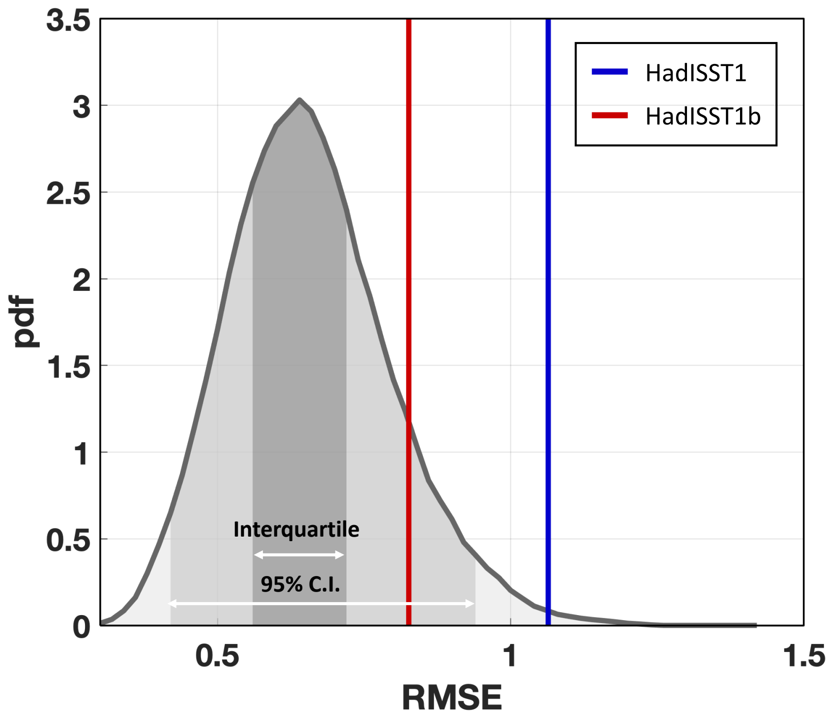


**Extended Data Fig. 2. RMSE between observed and ensemble-mean of simulated hurricane counts.** RMSEs are calculated using 15-year moving averaged hurricane counts. The null distribution (gray shading) is reconstructed using a Monte Carlo method by realizing only atmospheric internal variability, $\epsilon_i$, errors associated with uncertain groupwise corrections, $\frac{\mathrm{d}\mathbf{F}}{\mathrm{dT}}\epsilon_{\mathrm{T}}$, and errors in historical hurricane adjustment, $\epsilon_o$, following Eq. 1. Whereas the RMSE with HadISST1 (blue) is higher than the 99th percentile of the null distribution, the RMSE with HadISST1b (red) is the 90th percentile and becomes consistent with the null distribution.

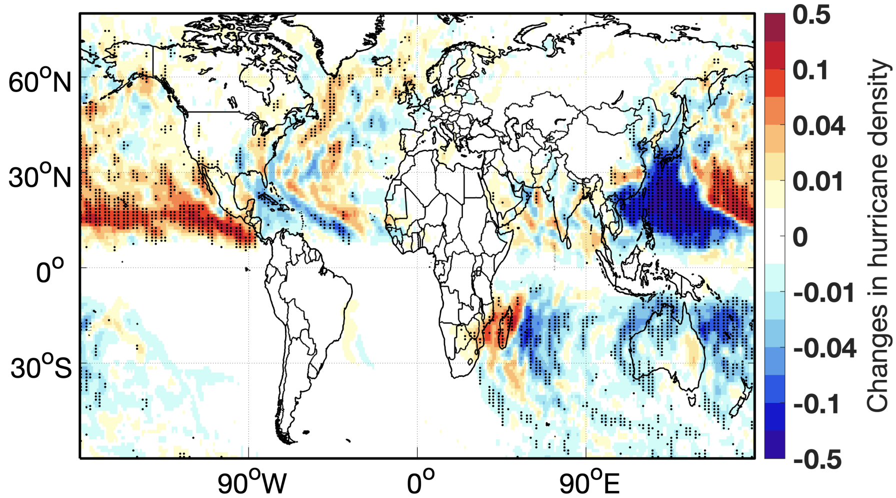


**Extended Data Fig. 3. Changes in hurricane track density in the RCP4.5 scenario.** Results are based on time-slice simulations (see methods). Whereas the control simulation is prescribed with 1982-2005 climatology in HadISST1, the RCP4.5 simulation implement increases in radiative forcing in the RCP4.5 scenario[46] and 2081-2100 SST warming over and 17 CMIP5 coupled models[34]. 50 years of data are collected for each simulation and dots denote significant changes in hurricane density ($P$ <0.05, two-sample t-test, N = 50).

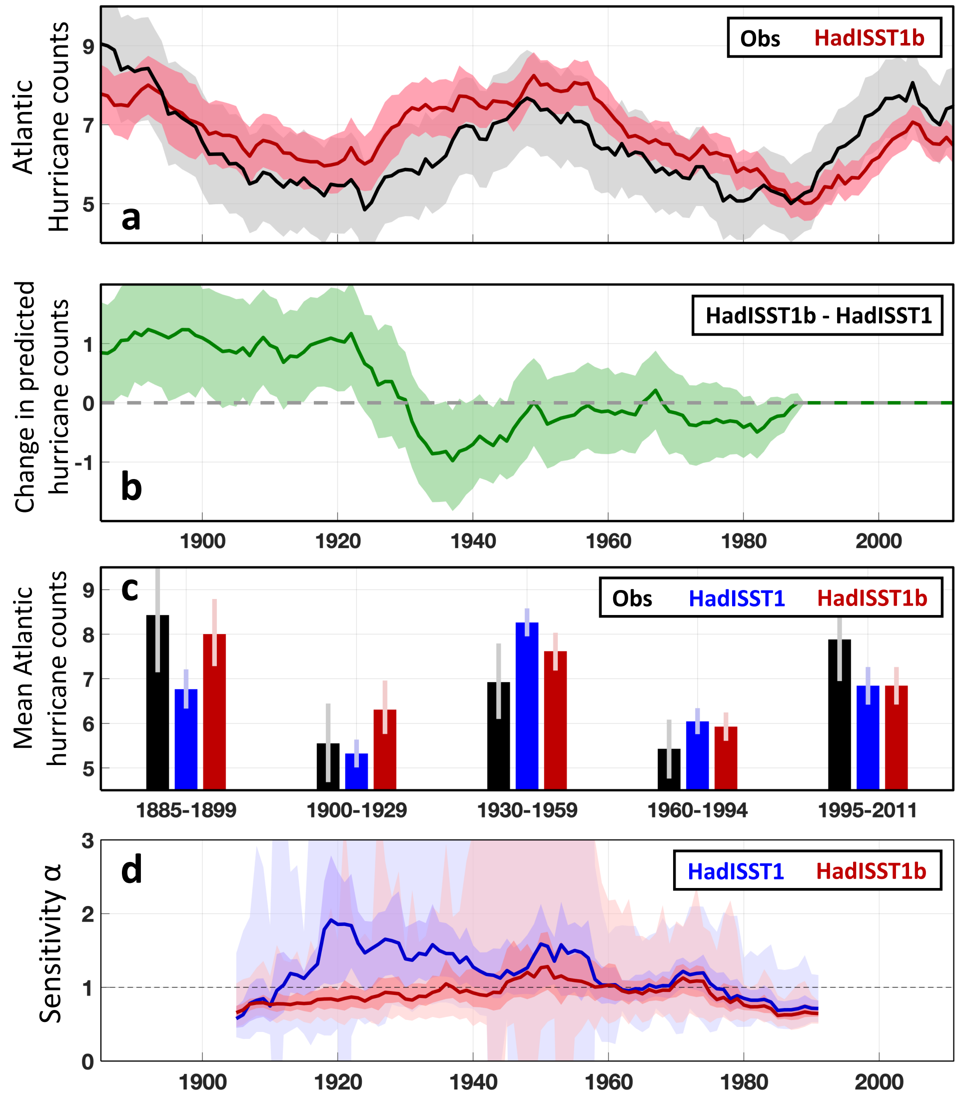


**Extended Data Fig. 4. Same as Fig. 1 but with SST corrections omitted after 1981.** To estimate the sensitivity associated with turning off groupwise bucket SST corrections in the satellite era, HadISST1b-based simulations since 1982 are replaced by simulations with HadISST1. Individual panels are as Fig. 1**b-d** and Fig. 4**a** in the main text. Improvements in reproduction skill with HadISST1b, together with a more stable relationship between Atlantic hurricane counts and SSTs, are robust to splicing data in the satellite era.

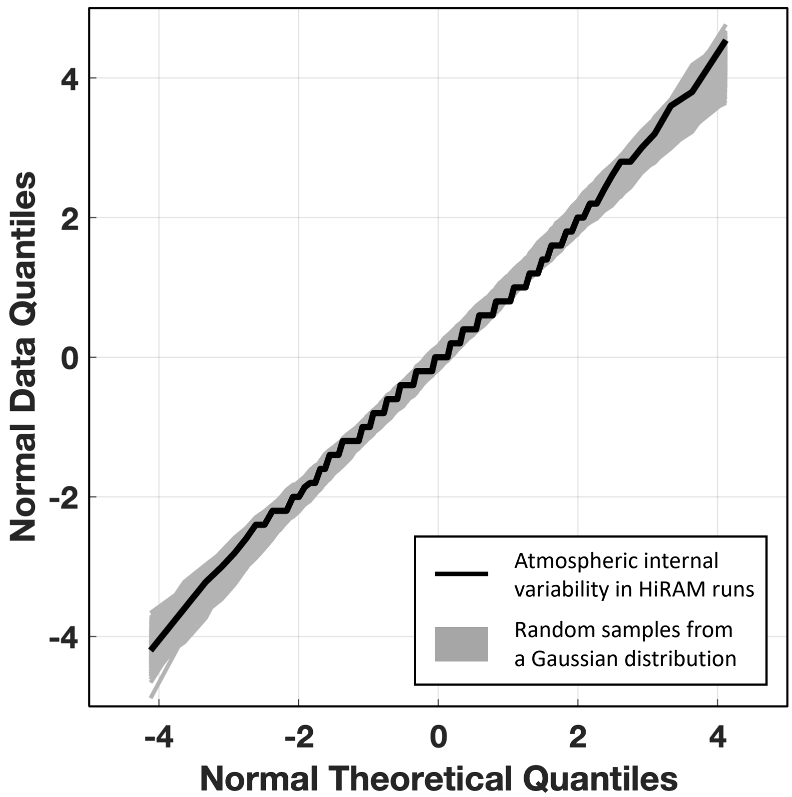


**Extended Data Fig. 5. Atmospheric internal variability in HiRAM can be approximated by a Gaussian distribution.** A quantile-quantile plot shows quantiles of atmospheric internal variability in HiRAM simulations against quantiles of a Gaussian distribution that has zero mean and a standard deviation of 1.97 (black). Atmospheric internal variability is quantified as the spread of HiRAM members around the ensemble mean. Gray shading show the range of quantile-quantile relationship wherein 1,000 random realizations of 1,480 samples are drawn from $N(0, 1.97^2)$. 1,480 is the total number of years in HadISST1 and HadISST1b HiRAM simulations and is the sample size of the black curve.

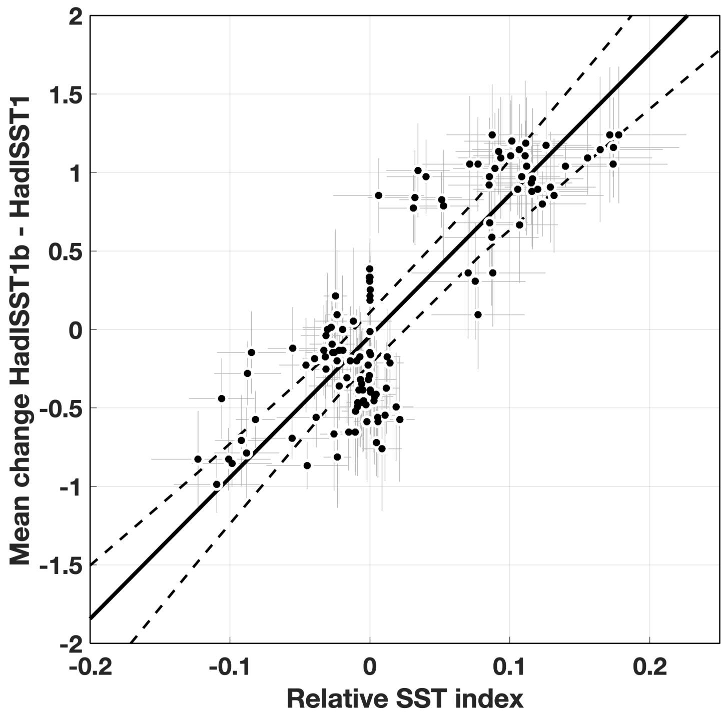


**Extended Data Fig. 6. Changes in simulated Atlantic hurricane counts versus changes in the relative SST index.** Changes in RSSTs (x-axis) are diagnosed from perturbed HadISST1b following ref.[14] (also see methods). Changes in simulated hurricane counts when specifying HadISST1b and HadISST1 in HIRAM simulations (green curve in Fig. 1c) are regressed against changes in the relative SST index (black curve in Figure 3). A York regression is used that accounts for uncertainties in hurricane counts (1 s.d. vertical bars) and RSST (1 s.d. horizontal bars). For display purposes (and as shown in Fig. 1c) hurricane counts are smoothed using a 15-year running average but smoothing does not effect the York regression when the resulting smaller uncertainties are accounted for.